Microresonator Brillouin Laser Gyroscope with Earth-Rotation-Rate Sensitivity

Myoung-Gyun Suh[1,2,†], **Yu-Hung Lai**[1,3,††], **Kerry J. Vahala**[1,†††]

[1]*T. J. Watson Laboratory of Applied Physics, California Institute of Technology, Pasadena, CA 91125, USA*
[2]*Present Address: Physics & Informatics Laboratories, NTT Research, Inc., Sunnyvale, CA 94085, USA*
[3]*Present Address: OEwaves Inc., 465 N. Halstead Str., Pasadena, CA 91107, USA*

[†]*mgsuh@ntt-research.com,* [††]*Yu-Hung.Lai@oewaves.com,* [†††]*vahala@caltech.edu*

Abstract:
Optical gyroscopes are widely used for precision navigation and there has been growing interest in the possibility of integrated optical gyroscopes. In this talk, we report a chip-based Brillouin laser gyroscope with Earth-rotation-rate sensitivity.

OCIS codes: (140.3945) Microcavities; (140.3370) Laser gyroscopes; (290.5900) Scattering, stimulated Brillouin.

Optical gyroscopes, which utilize Sagnac effect [1] for rotation sensing, are among the most accurate rotation measuring devices and are generally used for precision navigation systems. Modern optical gyroscopes enhance the Sagnac sensitivity using a long coil of optical fiber (fiber optic gyroscopes [2]) or by recirculation of laser wave within active ring resonators (ring laser gyroscope [3]). The enhanced performance is orders of magnitude better than that of micro-electro- mechanical-systems (MEMS) rotation sensors which are widely used in consumer electronics.

With the recent advance of integrated photonics, there has been growing interest in creation of chip-based optical gyroscopes [4]. Such integrated optical gyroscopes could enjoy the advantages of compactness and scalable manufacturing similar to MEMS gyroscopes. In addition, chip integration would offer extreme robustness in operation of optical gyroscopes. Compact or chip-based analogues of ring laser [5, 6], fibre-optic [7] and passive-resonant gyroscopes [8–10] have been reported so far.

In optical gyroscopes, the rotation sensitivity depends upon the linewidth of the beat note of counter-propagating laser waves, and the fundamental linewidth of lasers is of crucial importance on their performance. One way to achieve narrow laser linewidth is to harness Brillouin scattering process, which results from the interaction of an optical pump wave with acoustic phonons (Figure 1b). Brillouin process has been intensely studied in silica optical fibers [11] and more recently in photonic integrated circuits [12]. In particular, Brillouin process within a ring resonator can be used to generate stimulated Brillouin laser (SBL) showing sub-Hz fundamental linewidth limited by thermal occupation number of the resonator [6, 13, 14]. The application of SBLs for rotation sensing was demonstrated using optical fibers in the 1990s [15, 16] and integrated optics in recent years [5, 6]. Our initial work on chip-based Brillouin laser gyroscope was able to measure rotations rates as low as 22 $^\circ/h$ [5]. However, this earlier gyroscope demonstration used cascaded Brillouin lasers circulating in opposite directions and showed large bias drift.

In this talk, we report our recent demonstration of Brillouin Laser gyroscopes with improved performance [17]. In stead of using cascaded Brillouin lasers, counter-propagating Brillouin lasers are generated within the same cavity mode by pumping the resonator from both directions (Figure 1a). To avoid a rotation deadband induced by injection-locking via back scatter [3], nonzero pump detuning ($\Delta\nu_p < 1$ MHz) was introduced (Figure 1c). This near-degenerate mode of operation offers improved stability. The photo-detected beat note of the counter-propagating SBLs provides audio frequency readout signal, which relaxes requirements on processing electronics. The gyro readout beat frequency has a sub-Hz linewidth because of the narrow fundamental linewidth of each SBL due to the high optical Q factor of the resonator. Moreover, co-lasing of the clockwise and counter-clockwise Brillouin Stokes waves suppresses common-mode drift in the beat signal. The residual drift of the dual-SBL (counter-propagating) beat signal is further reduced by removing the correlated drift of the pump–SBL (co-propagating) beat frequency (Figure 2a) [17]. The Allan deviation of the gyro signal shows 0.068 $^\circ/\sqrt{h}$ angular random walk (ARW) and 3.6 $^\circ/h$ bias stability when using a 36 mm diameter resonator.

We also tested the performance of the Brillouin gyroscope by applying an external sinusoidal rotation. The gyroscope achieves a rotation amplitude sensitivity as low as 5 $^\circ/h$. In addition, by applying large rotation amplitudes, we confirm that the dispersion from the Brillouin lasing process introduces an additional mode-pulling correction factor to the conventional Sagnac factor. As a demonstration of gyroscope performance, the Earth's

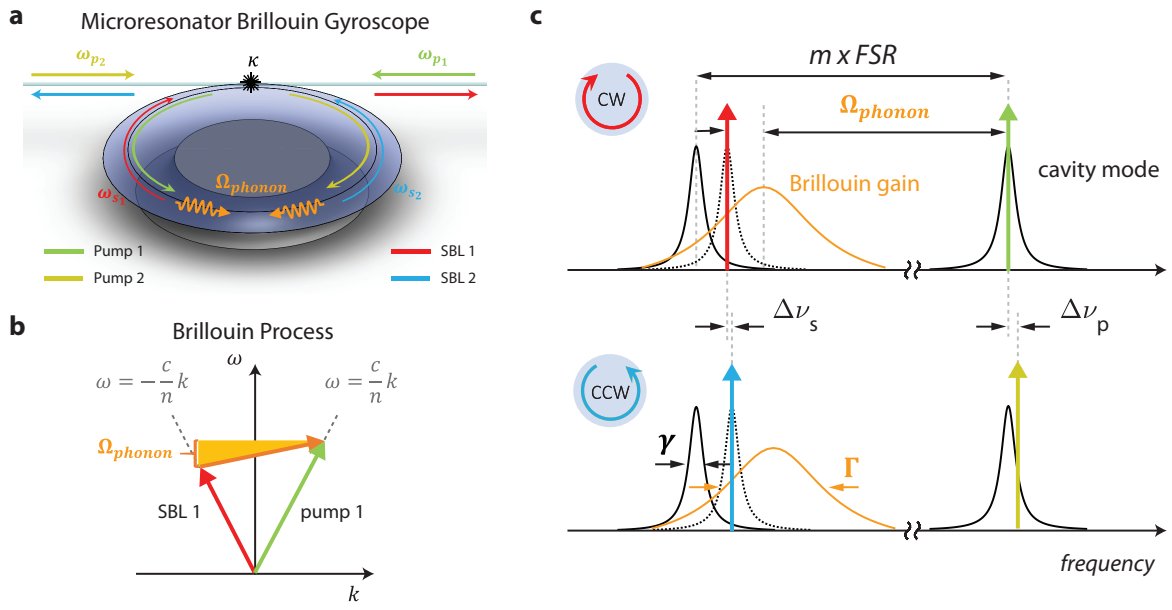

Fig. 1. **Principle of Microresonator-based Brillouin Laser gyroscope.** (a) Illustration of the dual stimulated Brillouin laser (SBL) process in a silica wedge-disk microresonator with a tapered fiber coupler. The green (yellow) solid curve represents pump 1 (pump 2) with angular frequency ω_{p_1} (ω_{p_2}) and the red (blue) solid curve represents SBL 1 (SBL 2) with angular frequency ω_{s_1} (ω_{s_2}). The orange wavy line represents the acoustic phonons with angular frequency Ω_{phonon}. (b) The energy and the momentum conservation constraints in the Brillouin process. A pump wave is scattered into a Stokes wave and an acoustic phonon. (c) For efficient Brillouin laser action, each Stokes mode (black with linewidth γ and separated from the pump by a multiple of the cavity FSR) lies within the Brillouin gain band (orange with linewidth Γ) which is shifted by $\Omega_{\text{phonon}} = 4\pi n c_s/\lambda_p$ (refractive index n, speed of sound in silica c_s and pump wavelength λ_p) relative to the pump frequency. Due to the offset $\Delta\nu_p$ in pump frequencies, dispersion from the Brillouin gain pulls the Stokes lasing modes by different amounts $\Delta\nu_s$ towards the gain center. In this work, the free spectral range(FSR) of the microresonator is $\sim$1.8 GHz to match the integer multiple ($m = 6$) of FSR with the Brillouin shift $\Omega_{\text{phonon}}/2\pi \approx 10.8$ GHz.

rotation was measured by switching the gyroscope axis between North and South directions (Figure 2b, upper panel). The gyroscope axis was also switched between East and West directions to verify no rotation (Figure 2b, lower panel). This demonstration of the Earth's rotation measurement using our Brillouin laser gyroscope shows the potential of chip-based optical gyroscopes in future inertial guidance systems.

Recent progress on integrated Brillouin lasers indicates further improvement in gyroscope performance is possible. Combination of higher optical Q-factor [18, 19] and higher Brillouin laser power through suppression of cascaded operation [20] enables further narrowing of fundamental laser linewidth, which could improve the gyroscope sensitivity. Operation of the gyroscope near an exceptional point can also enhance the Sagnac transduction factor [21, 22].

The authors thank the Defense Advanced Research Projects Agency (DARPA) for financial support (N66001-16-1-4046). We also gratefully acknowledge the infrastructure support provided by The Kavli Nanoscience Institute at Caltech.

References

1. G. Sagnac, "L'éther lumineux démontré par l'effet du vent relatif d'éther dans un interféromètre en rotation uniforme," CR Acad. Sci. **157**, 708–710 (1913).
2. H. C. Lefevre, *The fiber-optic gyroscope* (Artech house, 2014).
3. W. Chow, J. Gea-Banacloche, L. Pedrotti, V. Sanders, W. Schleich, and M. Scully, "The ring laser gyro," Rev. Mod. Phys. **57**, 61 (1985).

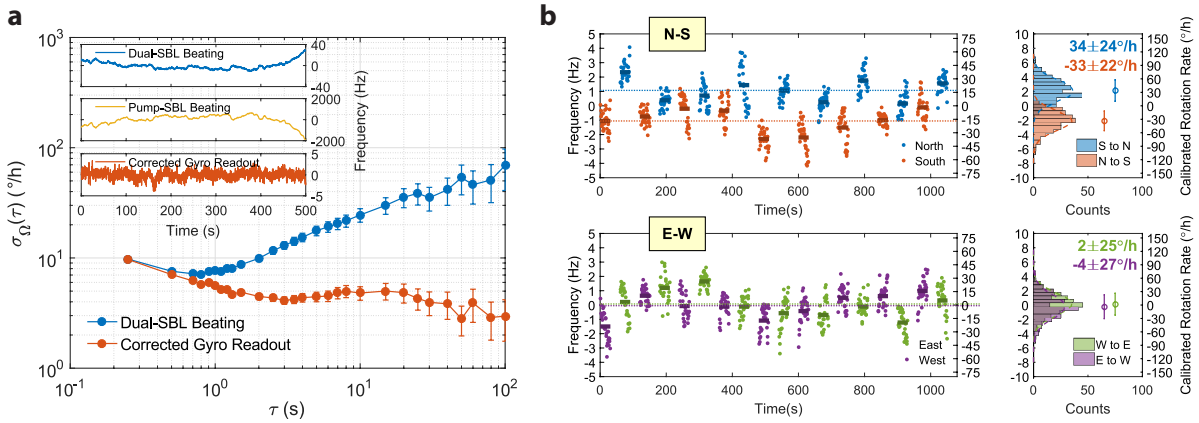

Fig. 2. **Performance of Brillouin Gyroscope** (a) Allan deviation of measured dual-SBL beatnote before and after drift compensation. Inset shows raw data used in these measurements. (b) Sagnac shift frequency versus time while the axis of the gyroscope is switched between North and South (N-S, upper panel) and East and West (E-W, lower panel) with $\Delta\nu_s < 0$ ($\Delta\nu_p$ = -500kHz). The resulting angular-rate change for N-S is close to twice the Earth's rotation rate ($2\times15^\circ/\mathrm{h}$), while the E-W measurement shows near zero change (histograms at the right panel). Both measurements show similar residual long-term drift from the environment.

4. F. Dell'Olio, T. Tatoli, C. Ciminelli, and M. N. Armenise, "Recent advances in miniaturized optical gyroscopes," J. Eur. optical society-Rapid publications **9** (2014).
5. J. Li, M.-G. Suh, and K. Vahala, "Microresonator brillouin gyroscope," Optica **4**, 346–348 (2017).
6. S. Gundavarapu, G. M. Brodnik, M. Puckett, T. Huffman, D. Bose, R. Behunin, J. Wu, T. Qiu, C. Pinho, N. Chauhan *et al.*, "Sub-hertz fundamental linewidth photonic integrated brillouin laser," Nat. Photonics **13**, 60–67 (2019).
7. S. Gundavarapu, M. Belt, T. A. Huffman, M. A. Tran, T. Komljenovic, J. E. Bowers, and D. J. Blumenthal, "Interferometric optical gyroscope based on an integrated si 3 n 4 low-loss waveguide coil," J. Light. Technol. **36**, 1185–1191 (2018).
8. W. Liang, V. S. Ilchenko, A. A. Savchenkov, E. Dale, D. Eliyahu, A. B. Matsko, and L. Maleki, "Resonant microphotonic gyroscope," Optica **4**, 114–117 (2017).
9. J. Zhang, H. Ma, H. Li, and Z. Jin, "Single-polarization fiber-pigtailed high-finesse silica waveguide ring resonator for a resonant micro-optic gyroscope," Opt. letters **42**, 3658–3661 (2017).
10. P. P. Khial, A. D. White, and A. Hajimiri, "Nanophotonic optical gyroscope with reciprocal sensitivity enhancement," Nat. Photonics **12**, 671–675 (2018).
11. E. Ippen and R. Stolen, "Stimulated brillouin scattering in optical fibers," Appl. Phys. Lett. **21**, 539–541 (1972).
12. B. J. Eggleton, C. G. Poulton, P. T. Rakich, M. J. Steel, and G. Bahl, "Brillouin integrated photonics," Nat. Photonics **13**, 664–677 (2019).
13. J. Li, H. Lee, T. Chen, and K. J. Vahala, "Characterization of a high coherence, brillouin microcavity laser on silicon," Opt. express **20**, 20170–20180 (2012).
14. M.-G. Suh, Q.-F. Yang, and K. J. Vahala, "Phonon-limited-linewidth of brillouin lasers at cryogenic temperatures," Phys. review letters **119**, 143901 (2017).
15. R. Kadiwar and I. Giles, "Optical fibre brillouin ring laser gyroscope," Electron. letters **25**, 1729–1731 (1989).
16. F. Zarinetchi, S. Smith, and S. Ezekiel, "Stimulated brillouin fiber-optic laser gyroscope," Opt. letters **16**, 229–231 (1991).
17. Y.-H. Lai, M.-G. Suh, Y.-K. Lu, B. Shen, Q.-F. Yang, H. Wang, J. Li, S. H. Lee, K. Y. Yang, and K. Vahala, "Earth rotation measured by a chip-scale ring laser gyroscope," Nat. Photonics **14**, 345–349 (2020).
18. L. Wu, H. Wang, Q. Yang, Q.-x. Ji, B. Shen, C. Bao, M. Gao, and K. Vahala, "Greater than one billion q factor for on-chip microresonators," Opt. Lett. **45**, 5129–5131 (2020).
19. M. W. Puckett, K. Liu, N. Chauhan, Q. Zhao, N. Jin, H. Cheng, J. Wu, R. O. Behunin, P. T. Rakich, K. D. Nelson *et al.*, "422 million intrinsic quality factor planar integrated all-waveguide resonator with sub-mhz linewidth," Nat. communications **12**, 1–8 (2021).
20. H. Wang, L. Wu, Z. Yuan, and K. Vahala, "Towards milli-hertz laser frequency noise on a chip," arXiv preprint arXiv:2010.09248 (2020).
21. Y.-H. Lai, Y.-K. Lu, M.-G. Suh, Z. Yuan, and K. Vahala, "Observation of the exceptional-point-enhanced sagnac effect," Nature **576**, 65–69 (2019).
22. H. Wang, Y.-H. Lai, Z. Yuan, M.-G. Suh, and K. Vahala, "Petermann-factor sensitivity limit near an exceptional point in a brillouin ring laser gyroscope," Nat. communications **11**, 1–6 (2020).